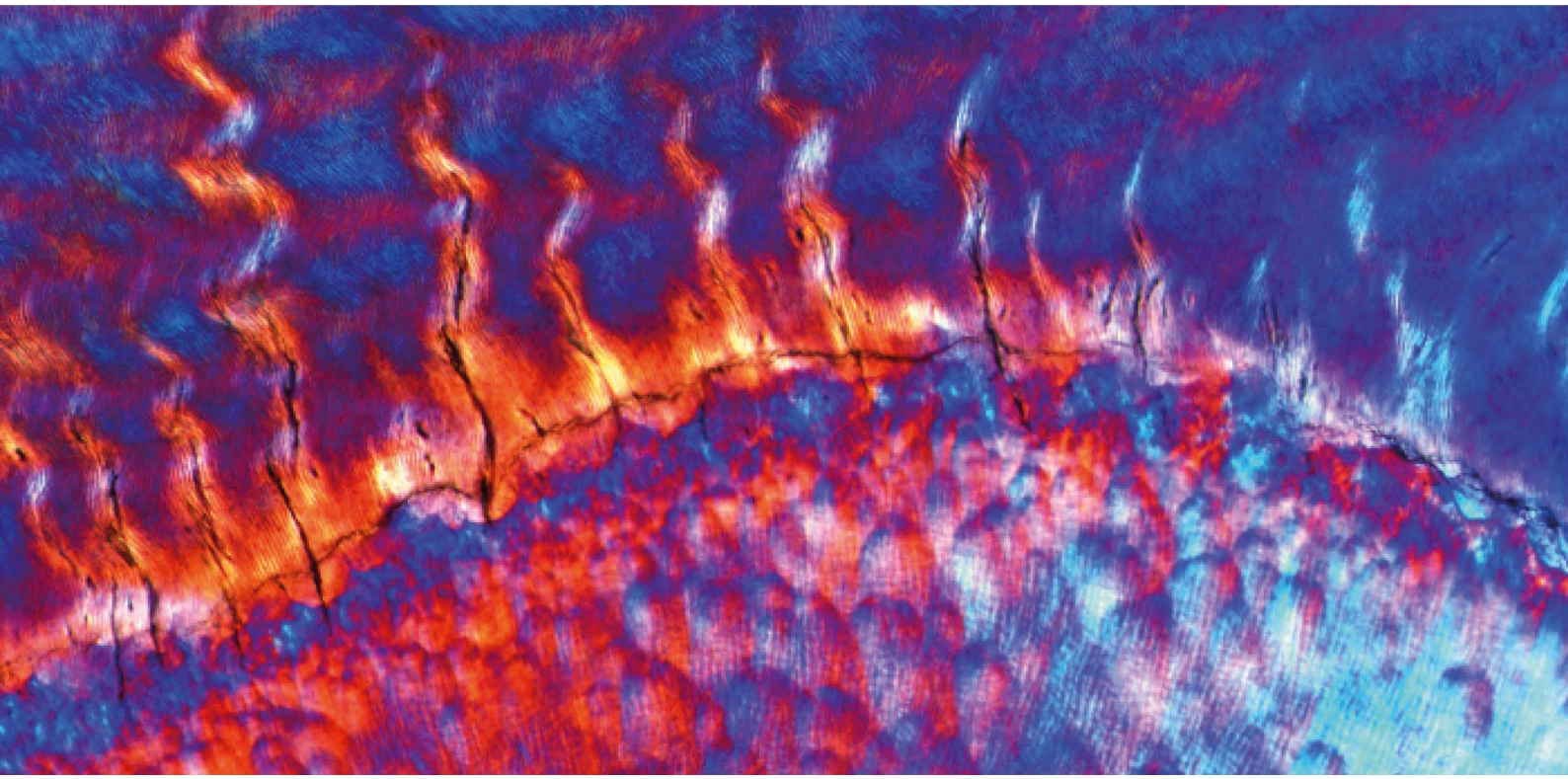

Timothy G. Bromage
Yusuf M. Juwayeyi
Igor Smolyar
Bin Hua
Santiago Gomez
Vincent J. Scaringia
Sydnee Chavise
Premsai Bondalapatif
Khushmit Kaurf
John Chisig

Signposts ahead: Hard tissue signals on rue Armand de Ricqlès

General palaeontology, systematics and evolution

Comptes rendus Palevol 10, 499–507, 2011

C. R. Palevol 10 (2011) 499–507

Contents lists available at ScienceDirect

Comptes Rendus Palevol

www.sciencedirect.com

General palaeontology, systematics and evolution

Signposts ahead: Hard tissue signals on rue Armand de Ricqlès

Poteaux indicateurs devant : signaux sur les tissus durs dans la rue Armand de Ricqlès

Timothy G. Bromage [a,*], Yusuf M. Juwayeyi [b], Igor Smolyar [c], Bin Hu [a], Santiago Gomez [d], Vincent J. Scaringi [a], Sydnee Chavis [e], Premsai Bondalapati [f], Khushmit Kaur [f], John Chisi [g]

[a] *Department of Biomaterials and Biomimetics, New-York University College of Dentistry, 345 East 24th Street, 10010-4086, New-York, USA*
[b] *Department of Anthropology, Long Island University, Brooklyn, 11201, New-York, USA*
[c] *Ocean Climate Laboratory, National Oceanic and Atmospheric Administration, Silver Spring, 20910 Maryland, USA*
[d] *Department of Pathological Anatomy, University of Cadiz, Cadiz, Spain*
[e] *University of Maryland, College Park, Maryland, USA*
[f] *Plainview-Old Bethpage John F. Kennedy High School, Plainview, New-York, USA*
[g] *Department of Haematology, University of Malawi College of Medicine, Blantyre, Malawi*

ARTICLE INFO

Article history:
Received 3 December 2010
Accepted after revision 15 February 2011
Available online 19 April 2011

Written on invitation of the Editorial Board

Keywords:
Enamel striae of Retzius
Lamellar bone
Growth rhythms

ABSTRACT

Of the major contributions to our understanding of the skeleton made by Armand de Ricqlès is the notion that within the microanatomy of bone we may observe "signals", some relating to phylogeny, and others to aspects of growth, function, and physiology. We are motivated to follow this road, as it were, and read the "signposts" along the way. Incremental structures are such signposts, representing biological rhythms as successive forming fronts in enamel and bone. A long period rhythm in humans, which occurs on average every eight to nine days, is observed in enamel as the stria of Retzius and in bone as the lamella. Because lamellae are formed within defined periods of time, quantitative measures of widths of individual lamellae provide time-resolved growth rate variability. Results obtained on primary incremental lamellar bone from midshaft femur histological sections of sub-Saharan Africans of Bantu origin and known life history reveal environmental effects heretofore unknown.

Mots clés :
Stries d'émail de Retzius
Os lamellaire
Rythmes de croissance

RÉSUMÉ

Une des contributions majeures d'Armand de Ricqlès est l'idée que la microstructure des os renferme des signaux sur la phylogénie, la croissance, les fonctions, et la physiologie. Nous souhaitons suivre cette voie et ainsi lire les signaux qui la jalonnent. Les structures de croissance sont de tels signaux ; elles représentent les rythmes biologiques par des vagues de dépôts dans l'émail et l'os. Un rythme de longue période, de huit à neuf jours en moyenne, est observé dans l'émail sous forme des stries de Retzius et dans l'os sous forme de lamelles. Puisque ces lamelles se forment pendant des périodes définies, des mesures quantitatives de l'épaisseur des lamelles fournissent de l'information détaillée sur la variation du taux de croissance. Des résultats ainsi obtenus sur la croissance de l'os lamellaire à partir de sections de la mi-diaphyse du fémur d'Africains sub-sahariens d'origine Bantoue et d'histoire de vie connue révèlent des effets environnementaux précédemment inconnus.

* Corresponding author.
E-mail address: tim.bromage@nyu.edu (T.G. Bromage).

1631-0683/$ – see front matter © 2011 Académie des sciences. Published by Elsevier Masson SAS. All rights reserved.
doi:10.1016/j.crpv.2011.01.009

1. Introduction

Of the major contributions to our understanding of the skeleton made by Armand de Ricqlès is the notion that within the microanatomy of bone, we may observe "signals", some relating to phylogeny, and others to aspects of growth, function, and physiology (de Ricqlès, 1976). We are motivated to follow this road, as it were, and read the "signposts" along the way. Incremental structures are such signposts, representing biological rhythms as successive forming fronts in enamel and bone. In particular, a long period rhythm in humans, which occurs on average every eight to nine days, may be observed in enamel as the stria of Retzius and in bone as the lamella (Bromage et al., 2009). Lamellar bone is thus an incremental tissue, which, when calibrated in time and measured appropriately, may reveal growth rate variability attributable to endogenous and exogenous factors. In this communication, we shall concentrate on variation attributable to environmental phenomena that are observable in primary lamellar bone from midshaft femur histological sections of sub-Saharan Africans of Bantu origin and known life history.

1.1. Background

Bone forming cells, the osteoblasts, secrete their organic matrix in discrete tissue patterns, which frequently include formation of the lamella, a fundamental microanatomical unit of bone observed in the postnatal tissues of many vertebrate taxa (de Ricqlès et al., 1991; Enlow and Brown, 1956–1958). The lamella is characterized in histological thin sections by a highly oriented band of collagen separated from adjacent bands by an interlamellar zone of less oriented collagen (Ascenzi et al., 1967), resulting in the discrimination of one lamella from the next in polarized light. Lamellar bone is strikingly incremental in appearance, but the periodic formation of lamellae is the subject of only two preliminary reports (Okada and Mimura, 1940; Shinoda and Okada, 1988) In this early research, a 24-hour rhythm was recorded for the formation of one lamella in three small mammals (Wistar rats with a mean body weight of 124 g, Asiatic chipmunks with a mean body weight of 62 g, Japanese white rabbits with a mean body weight of 860 g) and a longer but uncertain rhythm in one larger mammal (a Beagle dog with a body weight of 11.3 kg).

Fortunately, the possibility now exists to assign a timescale to lamellar bone using calibrated enamel increments that, in mammalian teeth, exhibit incremental features representing successive forming fronts of enamel at varying time scales (Bromage et al., 2009). There exists a daily period, which, by light microscopy, is recognized as a "cross striation", and there is a long period "stria of Retzius" that, in humans, occurs every ca. eight to nine days on average, and measured as the number of cross striations between adjacent striae. The number of daily increments between striae is the repeat interval (RI), which is identical for all teeth of an individual, yet variable between and occasionally within a species (Fitzgerald, 1998). Species variability in RI reflects a statistically significant and positive relationship with body size, explained by the discovery that the period responsible for RI formation is one and the same as that required to form one increment of bone, the lamella, the fundamental – if not archetypal – unit of bone, (Bromage et al., 2009). Lamellae of known formation time nevertheless vary in width, and thus provide time-calibrated growth rate variability (variability in width along lengths of single lamellae is an aspect of lamellar anisotropy, which is subject to statistical evaluation and that is briefly described in Light Microscopy Imaging and Analysis below).

We aim to apply novel image analytical methods for characterizing periodic textures manifest in lamellar bone incremental patterns and illustrate growth rate variability for as many as six years of continuously forming primary incremental lamellar bone from midshaft femur histological sections of sub-Saharan Africans of Bantu origin and known life history.

2. Materials and methods

2.1. Hard tissue specimens and life history

Midshaft segments of approximately 10 cm in length were cut from cadaveric femurs on the right side of twelve people of Bantu origin following the gross anatomy program of the Department of Anatomy of the University of Malawi College of Medicine (UMCOM). One half-mandible from the right side was also acquired from seven of these individuals by dissecting the mandibular condyle free from the temporomandibular joint, and sawing the symphysis through to preserve the right central lower incisor.

Following cadaver selection, UMCOM staff administered a questionnaire to next of kin, in which medical, social, economic and life history information was sought. The medical history is particularly relevant to disease risk in Malawi. Social history information relates to living conditions and employment. We also acquired common life history variables, such as age, sex, height, and weight (mass). In addition, questions were developed to solicit information relating to autonomic function.

2.2. Specimen preparation

Bone and tooth specimens were transferred to the New-York University College of Dentistry and cleaned of non-mineralised organic components with daily changes of fresh 1% Terg-a-Zyme (Alconox, New-York) enzyme detergent at 50 °C until clean (Boyde, 1984). A ca. 1.0-cm block was sawn from the midportion of each femur and subjected to further enzyme detergent treatment until there were no visible non-mineralised organics.

Bone and tooth specimens were subject to graded ethanol substitution and then 50:50 isopropanol:heptane reflux in a Soxhlet apparatus for seven to 14 days, and then polymethylmethacrylate (PMMA) substitution and embedding. Cured PMMA blocks were hand-ground on 1200 grit paper with a Buehler Handimet II (Buehler, IL) along their sides facing midshaft, mounted to a strain-free Exakt plastic slide (Exakt Technologies, OK), thin-sectioned with the Exakt 300 CP Band System, and polished on an automated Exakt 400 CS Grinding System with 1200 grit paper until plane-parallel at ca. 50-μm thick. Mounted histological

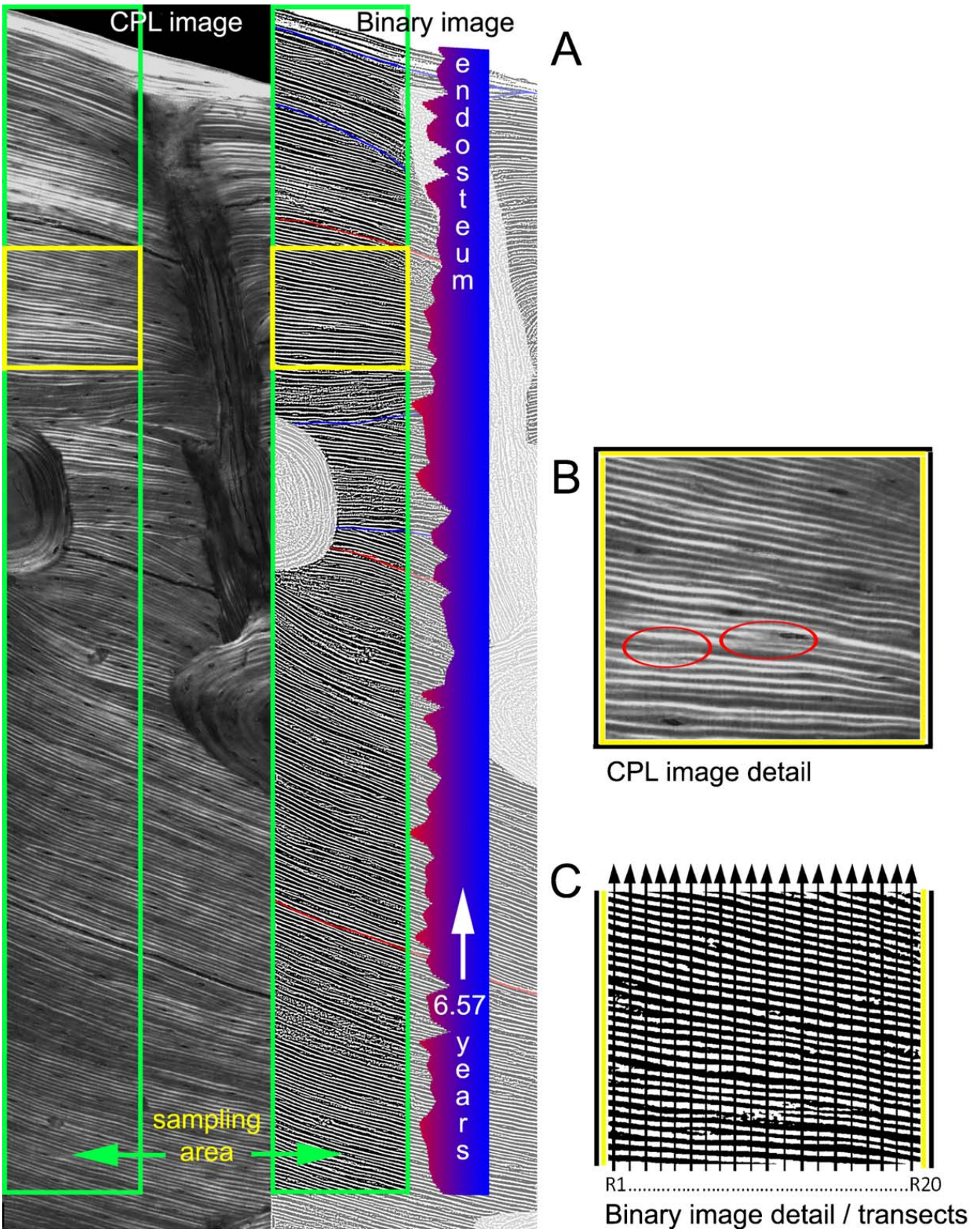

Fig. 1. (A) CPL and Binary images of primary lamellar bone of individual 08-02, a businessman (Fig. 3) (Field Width ca. 200 μm each image). The area analysed for growth rate variability is enclosed within a green square. Red lines on the binary image are dehydration cracks, while blue lines represent instances in which a cessation, or reversal, in growth occurred. To the right of the binary image is a coloured diagram of growth rate variability in which growth rate peaks to the left and decreases to the right from the bottom to the top (endosteum) of the image for a duration of over ca. 6.5 years. (B) CPL image detail from yellow inset in (A), in which anisotropic lamellae are illustrated in marked red oval areas. (C) Binary image detail with transects overlain in preparation for the measurement protocol.

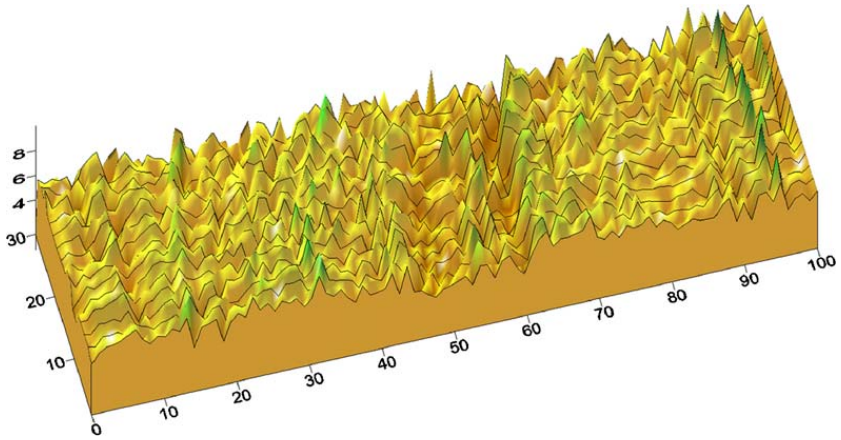

Fig. 2. 3D chart of processed growth rate variability of individual 08-02, a businessman (Fig. 3). Growth rate is shown on the *Z*-axis (scale in micrometers), while time is represented on the X-axis from left to right (scale is the proportion of lamellae during the time course; the front surface of this 3D chart is illustrated vertically in Fig. 1A). The Y-axis represents decreasing error in the measurements of lamellar widths from back to front (Smolyar and Bromage, 2004 for an explanation of the method).

Fig. 2. Diagramme 3D de la variabilité de la vitesse de croissance traité pour l'individu 08-02, homme d'affaire (Fig. 3). La vitesse de croissance est représentée sur l'axe *Z* (échelle en μm), tandis que le temps l'est sur l'axe *X* de la gauche vers la droite (l'échelle est la proportion de lamelles au cours du temps : la surface frontale de ce diagramme 3D est illustrée verticalement sur la Fig. 1A). L'axe *Y* représente l'erreur décroissante sur les mesures de largeur des lamelles, de l'arrière vers l'avant (Smolyar et Bromage, 2004 pour une explication de la méthode).

sections were polished on a Buehler Ecomet 3 to produce a 1-μm surface finish.

2.3. Light microscopy imaging and analysis

Histological sections were cover-slipped with immersion oil and imaged in circularly polarized transmitted light (CPL) using a Leica-Leitz DMRXE Universal Microscope configured with a Marzhauser motorized stage and CPL filters and Leica PL Fluotar 40/0.70 (enamel) and PL Fluotar 20/0.50 (bone) objective lenses (Leica Microsystems, IL). CPL image montages were acquired using Syncroscopy Montage Explorer software (Synoptics, MD). Evaluation of the number of daily increments between adjacent striae of Retzius – the repeat interval (RI) – was performed on XY montages of whole sections from seven of twelve individuals.

Monochrome CPL montages of primary lamellar bone at periosteal and endosteal locations around the femur midshaft cortex were acquired in raster format. Multiple montages of varying illumination intensity over same X-Y fields of view were combined into single high dynamic range (HDR) image and "tone-mapped" using Photomatix Pro software (v. 3.2; HDRSoft, Montpellier, France) bringing dark lamellar domains into view [28]. Tone-mapped images were rendered as a binary using Adobe Photoshop CS3 (San Jose, CA) (Fig. 1).

To formalize the incremental pattern, we applied a discrete model based upon the parameterisation of incremental structure (Smolyar and Bromage, 2004). An in-house program written for Microsoft Excel 2007 (Redmond, WA) was used to import binary images and semi-automatically plot transects perpendicular to the direction of growth. Transects generated intersections with lamellae, and each intersection was given an XY coordinate. Measurements were then made (in micrometers) between all adjacent coordinates along transects. However, a typical field of view reveals that lamellae are of varying width and contain breaks and confluences along their lengths, and thus represent an anisotropic pattern, which must be considered when making measurements of lamellar widths. Anisotropy has an impact on the accuracy of measurements and, hence, evaluations of growth rate variability were assessed by calculations of entropy and structural anisotropy, which we accomplished by evaluating all alternate possible relationships between lamellae crossed by adjacent transects; these statistics may be used to determine confidence in the results when anisotropy is severe (Smolyar and Bromage, 2004, for a complete description of the method; see Fig. 1 for examples of lamellar bone anisotropy). A graphic representation of growth rate variability with the most statistical confidence is an outcome of this analysis, which by example, we illustrate in Figs.1 and 2.

2.4. Duration of lamellar development

We used the RI to calculate the total duration of lamellar development for each CPL montage. There were five individuals in the study sample that did not have enamel

Fig. 1. (A) Images binaires et CPL d'un os lamellaire primaire de l'individu 08-02, homme d'affaire (Fig. 3) (largeur du champ environ 200 μm pour chaque image). La surface analysée pour la variabilité de la vitesse de croissance est comprise dans un rectangle vert. Les lignes rouges sur l'image binaire représentent des fentes de déshydratation, tandis que les lignes bleues représentent des exemples d'arrêt ou d'inversion de croissance. Sur la partie droite de l'image binaire, se trouve un diagramme coloré, de variabilité de la vitesse de croissance sur lequel la vitesse de croissance continue à gauche et décroît à droite, de la base vers le haut (endosteum) de l'image, pour une durée d'environ 6,5 ans. (B) Image CPL provenant de l'encart jaune en (A), dans laquelle les lamelles anisotropes apparaissent dans des aires ovales bordées de rouge. (C) Détail de l'image binaire, avec les transects en préparation pour le protocole de mesure.

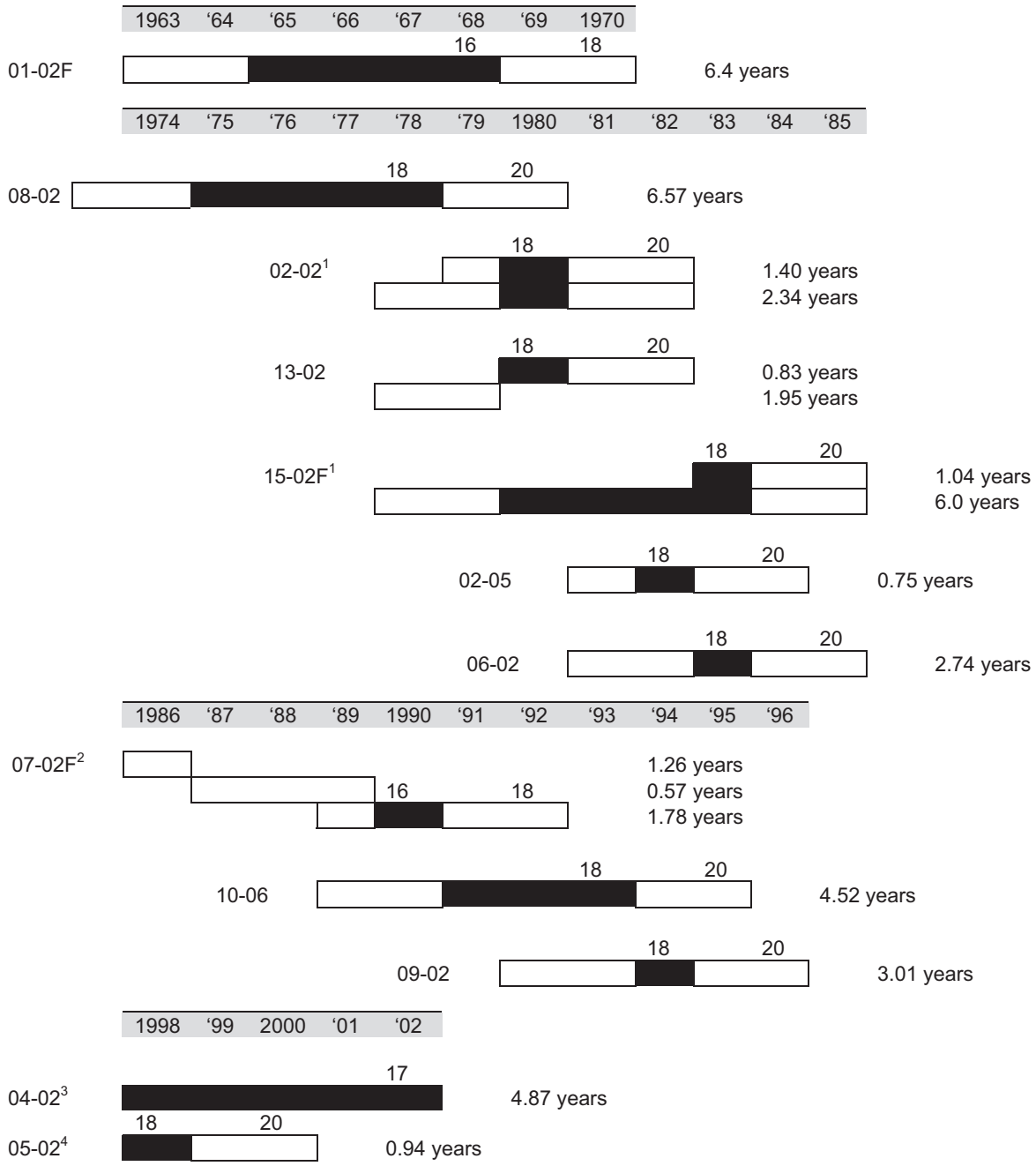

Fig. 3. Lamellar bone development and approximate alignment in real years. Bars/boxes for each individual in the study sample appear below years (shaded). Specimen numbers at left of boxes/bars include an "F" for females, otherwise individuals are male. Black bars indicate the duration of lamellar development for years most likely to be represented. Age ranges at skeletal maturity is given above bars/boxes, and total lamella formation time is given at right for each histological section evaluated based on 9- and 8-day lamellar formation rate for females and males respectively. Open boxes at left and right of black bars indicate the duration of lamella formation if maturing early or late respectively.[1] Two CPL montages were assessed for this individual. [2] Cement lines indicate arrested growth for two periods of lamellar deposition, indicated as open boxes of 1.26 and 0.57 years duration. [3] This individual was still growing at the time of death.[4] This individual was still growing at the time of death if late maturing.

Fig. 3. Développement de l'os lamellaire et alignement approximatif en années réelles. Les barres/boîtes caractérisant chaque individu étudié apparaissant sous les années (ombrées). Les codes des échantillons, à la gauche des barres/boîtes incluent un « F » pour les individus féminins ; sinon les individus sont des mâles. Les barres noires indiquent la durée du développement lamellaire pour les années à représenter de préférence. Les échelles d'âge lors de la maturité squelettique sont données au-dessus des barres/boîtes et la durée totale de formation des lamelles est fournie à droite pour chaque coupe histologique, évaluée à partir d'une vitesse de formation lamellaire de neuf et huit jours, pour les femmes et les hommes, respectivement. Les boîtes blanches à gauche et à droite des barres noires indiquent la durée de formation des lamelles, si la maturation est précoce ou tardive respectivement. [1] Deux montages CPL ont été évalués pour cet individu. [2] Les lignes de cémentation indiquent un arrêt de croissance pour deux périodes de dépôt lamellaire, représentées par deux boîtes blanches de durée 1,26 et 0,57 an. [3] Cet individu était encore en cours de croissance au moment de sa mort. [4] Cet individu était encore en cours de croissance, au moment de sa mort, si la maturation était tardive.

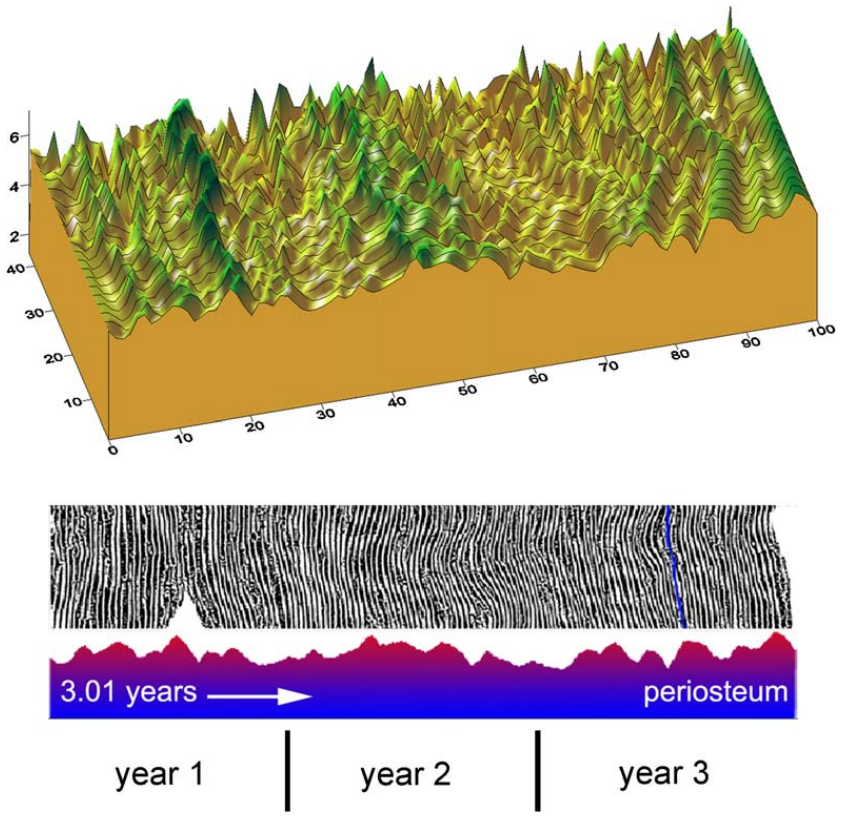

Fig. 4. (Top) Growth rate is shown on the *Z*-axis (scale in micrometers), while time is represented on the *X*-axis from left to right (scale is the proportion of lamellae during the time course). The *Y*-axis represents decreasing error in the measurements of lamellar widths from back to front (Smolyar and Bromage, 2004 for an explanation of the method). (Bottom) Binary image of primary lamellar bone of individual 09-02, a rural fisherman (Fig. 3) (Field Height ca. 200 μm). Growth rate is shown on the *Y*-axis while time is represented on the X-axis. Three cycles of growth occur in three years, which are roughly indicated in segments at the bottom of the figure.

Fig. 4. À la partie supérieure : la vitesse de croissance est représentée sur l'axe *X* de la gauche vers la droite (l'échelle est la proportion de lamelles au cours du temps). L'axe *Y* représente l'erreur décroissante sur les mesures de largeur des lamelles de l'arrière vers l'avant (Smolyar et Bromage, 2004 pour une explication de la méthode). À la partie inférieure : image binaire d'un os lamellaire primaire de l'individu 09-02. pêcheur rural (Fig. 3) (Hauteur du champ environ 200 μm). La vitesse de croissance est représentée sur l'axe Y, tandis que le temps l'est sur l'axe *X*. Trois cycles de croissance se produisent en trois ans, indiqués par des segments au bas de la figure.

specimens, and thus for them we used calculations of average RI values obtained from a large sample of teeth from people of sub-Saharan African origin.

Because bone lamellae and/or their CPL montages are frequently anisotropic, it is not possible to calculate an unbiased number of lamellae and, thus, the duration of lamellar bone development. However, in the absence of an accepted protocol, each visible lamella was counted and despite the possible effects of anisotropy, based on our experience, we have assumed that our calculations were within 5% of the real time elapsed. To place the duration of lamellar bone development in approximate real time, we extrapolated the time to include known ranges of ages at skeletal maturity from studies of physical development in people of sub-Saharan African origin (Lewis et al., 2002; Loder et al., 1993). These studies provide information useful for estimating the average age of skeletal maturity among Malawians, which for girls is between 16 to 18 years and for boys is between 18 to 20 years. The alignment of lamellar bone development in real time included the possibility that any one individual may have matured either early or late in respect of age ranges at skeletal maturity for their sex (Fig. 3). An assumption that we must naturally make, and which forms the basis of our future studies, is that the last lamella formed at periosteal or endosteal margins in the principal direction of cortical growth (i.e. drift) is at or near to the time of skeletal maturity; comparisons of growth curves of people of sub-Saharan African origin with people of European origin described elsewhere suggest that this assumption has merit (Bromage et al., in press).

3. Results

Seven individuals of the twelve in our study sample included teeth for obtaining their RI. Six males were observed to have an RI of 8 days (02-02, 06-02, 08-02, 09-02, 10-06, and 13-02) and one female exhibited an RI of 9 days (15-02) (Fig. 3). To estimate RI for the remaining five specimens in the study sample, we calculated average values for a sample of 244 South Africans of African origin of known age and sex described previously (Reid and Dean, 2006). Raw data for this sample kindly provided by Don Reid (University of Newcastle) indicate that, while the sample range was 6 to 12 days, female RI tends to be longer (mode = 9; mean = 9.2) than the RI of males (mode = 8; mean = 8.6), in agreement with the suggestion of a sex difference in this sample by Smith (Smith et al., 2007) and with the values observed for the teeth in our study sample. Thus,

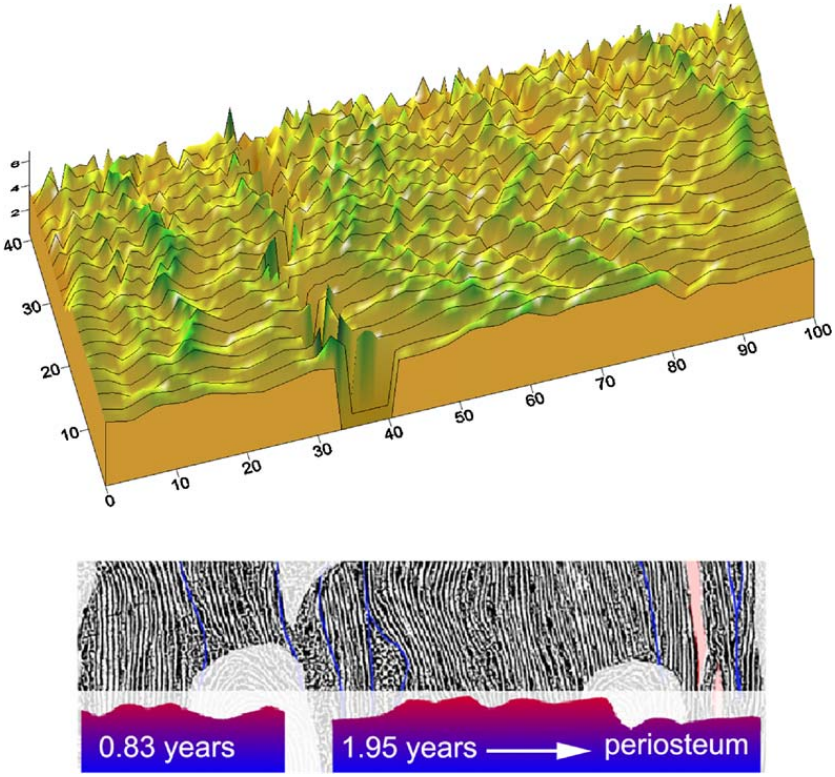

Fig. 5. (Top) Growth rate is shown on the *Z*-axis (scale in micrometers), while time is represented on the X-axis from left to right (scale is the proportion of lamellae during the time course). The Y-axis represents decreasing error in the measurements of lamellar widths from back to front (Smolyar and Bromage, 2004 for an explanation of the method). (Bottom) Binary image of primary lamellar bone of individual 13-02, a farmer (Fig. 3) (Field Height ca. 200 μm). Growth rate is shown on the *Y*-axis while time is represented on the *X*-axis. Low amplitude growth rate variability may reflect that this individual was a farmer who experienced a severe drought during the time represented by their primary lamellar bone deposition.
Fig. 5. À la partie supérieure : la vitesse de croissance est représentée sur l'axe *Z* (échelle en μm), tandis que le temps l'est sur l'axe *X*, de la gauche vers la droite (l'échelle est la proportion de lamelles au cours du temps). L'axe *Y* représente l'erreur décroissante sur les mesures de largeur des lamelles, de l'arrière vers l'avant (Smolyar et Bromage, 2004), pour une explication de la méthode). À la partie inférieure : image binaire de l'os lamellaire primaire de l'individu 13-02, un fermier (Fig. 3) (Hauteur du champ, environ 20 μm). La vitesse de croissance est représentée sur l'axe *Y*, tandis que le temps l'est sur l'axe X. La variabilité de faible amplitude du taux de croissance peut refléter que cet individu, un fermier a subi une sécheresse sévère, pendant le temps représenté par le dépôt d'os lamellaire primaire.

for determinations of the duration of lamellar bone development from all CPL montages, 9 days/lamella was used for females and 8 days/lamella was used for males. The durations of time represented by consecutive primary lamellar bone is provided in Fig. 3, which varies from 0.75 years to 6.57 years.

Most individuals in the study sample provided periodic growth rate variability in the approximate range of six to eight weeks. For instance, individual 08-02, an urban businessman, has a roughly eight-week oscillatory rhythm (Figs. 1 and 2) over 6.57 years between the extremes of 4 μm per lamella at the lowest rate of growth to 8 μm per lamella when growth was at its fastest. Attention to the characteristics of the original CPL and binary images for this individual should be noted, revealing several discontinuities; red lines on the binary image are dehydration cracks, which have no timeline significance, but blue lines represent instances in which a cessation or reversal in growth occurred for some unspecified period of time. This means that assessment of the duration of lamellar bone development for this image represents a minimum period of time.

Subjective annual periods are revealed in some cases. Individual 09-02, a rural fisherman, illustrates growth rate variability containing three low frequency oscillations in three years (Fig. 4). During this period, the minimum growth rate of this individual was 5 μm per lamella at the lowest rate of growth to 7 μm per lamella when growing their fastest.

We have also observed that the growth rate variability for two subsistence farmers is subjectively more flat, lacking growth spikes and relatively abrupt growth decelerations that characterize the fishermen, businessmen and women, sex workers, and the unemployed individuals in the UMCOM sample (e.g. individual 13-02; Fig. 5). During this period, a minimum of 4 μm per lamella was accrued at the lowest rate of growth and 6 μm per lamella at their fastest period of growth.

4. Discussion

Information about biological periodicities, environmental and/or physiological cycles, and growth perturbations are all potentially contained within growth rate variability studies of lamellar incremental patterns. Because lamellae are formed within defined periods of time, quantitative measures of widths of individual lamellae provide time-resolved growth rate variability with potential to reveal bone growth rhythms.

In the present study of humans of Bantu origin, for the first time we have observed striking lamellar growth rate rhythms, revealing heretofore unknown cycles at various length scales. The six to eight-weeks rhythm frequently identified (Figs. 1 and 2) does not presently align with any known endogenous physiological or exogenous environmental rhythm. However, the observance of an annual rhythm in some individuals (Fig. 4) is known to occur in mammals that live in seasonal environments and that experience yearly oscillations in resource availability (Klevezal, 1996). In the case of growth rate variability in the rural fisherman illustrated in Fig. 4, we have reason to question resource availability as a cause of the annual rhythm. This individual was male, 1.75 m in height, and weighing in at 82 kg when he died in 2002 at age 26. He was educated to Standard 8 (well above the average for Malawi, (Education Statistics, 2004) and his three favourite foods were reported to be chicken, beef, and pork. His income per month was well above the rural average at 30,000 Malawi Kwatcha, demonstrating affluence sufficient to afford these foods.

It is possible that, apart from resource variability, the fisherman's adolescence may nevertheless have been subject to the vagaries of seasonal change on annual timescales. For instance, he was reported to have had malaria twice yearly, occurrences of which commonly take place during the long wet season that extends from the beginning of November to the end of March. This seasonal rhythm is manifest in annual cycles of malaria, which is a metabolic cost severe enough to divert resources from growth to those necessary to survive the illness.

The low amplitude growth rate variability characterized by the two subsistence farmers is of great interest. This is contrary to the increased variability observed for people in other occupations. Both of these farmers were depositing primary lamellar bone whilst Malawi experienced the severe drought of 1980–1982: they are individuals 02-05 and 13-02 (Fig. 3). For instance, the widths of lamellae for the businessman varied from 4 to 8 μm (individual 08-02) and that of the fisherman from 5 to 7 μm (individual 09-02), whilst the farmer varied only from 4 to 6 μm (individual 13-02). Drought conditions are recognized to deleteriously affect the small farmer (Vogel et al., 2000), and we provisionally suggest that diminished growth rate variability is a characteristic of farmers prone to fluctuations in climate and who are less capable of ameliorating shortfalls and food instability. This would be particularly true for subsistence farming, which makes up the larger share of farming practices in Malawi, and because of their rural residence, we expect that this was the case for these two individuals.

The research presented here based on the histological analyses of skeletal (tooth and bone) remains of 12 Bantu individuals of known sex and life history, clearly shows that incremental lamellar bone is a unique signpost revealing long period growth rate variability heretofore unobserved in humans. They offer a glimpse of the potential for recognizing physiological and environmental rhythms and thus an opportunity to understand the larger ecological context in which an individual was living.

Acknowledgments

We acknowledge assistance from Maggie Ndhlove for following up the family histories of our UMCOM subjects. Support for SG's sabbatical at NYUCD was granted by the Ministerio de Educación, Spain. Summer research support for SC was provided by a University of Maryland 2010 Summer Internship Scholarship, and for VS it was provided by NYUCD Office of the Dean of Research Summer Research Program for incoming D1 students. This study was supported by a National Science Foundation grant in aid or research to TGB and YMJ (BCS-0741827) and by the 2010 Max Planck Research Award support of TGB's Hard Tissue Research Program in Human Paleobiomics. Finally, we thank Armand de Ricqlès for setting us onto the road and for teaching us how to read the signposts along the way. We are grateful to Michel Laurin and Jorge Cubo for the invitation to attend the symposium in Armand's honour and to present this paper.

References

Ascenzi, A., Bonucci, E., Bocciarelli, D.S., 1967. An electron microscope study on primary periosteal bone. J. Ultr. Res. 18, 605–618.

Boyde, A., 1984. Methodology of calcified tissue specimen preparation for SEM. In: Dickson, G.R. (Ed.), Methods of calcified tissue preparation. Elsevier, Amsterdam, pp. 251–307.

Bromage, T.G., Lacruz, R.S., Hogg, R., Goldman, H.M., McFarlin, S.C., Warshaw, J., Dirks, W., Perez-Ochoa, A., Smolyar, I., Enlow, D.H., Boyde, A., 2009. Lamellar bone is an incremental tissue reconciling enamel rhythms, body size, and organismal life history. Calcif. Tissue Int. 84, 388–404.

Bromage, T.G., Juwayeyi, Y.M., Smolyar, I., Hu, B., Gomez, S., Chisi, J. (in press). Enamel-calibrated lamellar bone reveals long period growth rate variability in humans. Proceedings of the 10th International Conference on the Chemistry and Biology of Mineralized Tissues, Carefree, Ariz., November 7–12, 2010. Cells Tissues Organs.

de Ricqlès, A., 1976. On bone histology of fossil and living reptiles, with comments on its functional and evolutionary significance. In: Bellairs, A.D.A., Cox, B. (Eds.), Morphology and biology of reptiles. Linnean Society of London and Academic Press, London, pp. 126–150.

de Ricqlès, A., Meunier, F., Castanet, J., Francillon-Vieillot, H., 1991. Comparative microstructure of bone. In: Hall, B. (Ed.), Bone-volume 3: bone matrix and bone specific products. CRC Press, Boca Raton, pp. 1–78.

Education Statistics, 2004. In: Government of Malawi.

Enlow, D.H., Brown, S.O., 1956–1958. A comparative histological study of fossil and recent bone tissues. Parts I-II. Tex. J. Sci. 8, 9, 10:405–443, 186–214, 187–230.

Fitzgerald, C.M., 1998. Do enamel microstructures have regular time dependency? Conclusions from the literature and a large-scale study. J. Hum. Evol. 35, 371–386.

Klevezal, G.A., 1996. Recording structures of mammals: determination of age and reconstruction of life history. A. Balkema, Rotterdam.

Lewis, C.P., Lavy, C.B.D., Harrison, W.J., 2002. Delay in skeletal maturity in Malawian children. J. Bone Joint. Surg. 84–B.

Loder, R.T., Estle, D.T., Morrison, K., Eggleston, D., Fish, D.N., Greenfield, M.L., Guire, K.E., 1993. Applicability of the Greulich and Pyle skeletal age standards to Black and White children of today. Am. J. Disease Child 147, 1329–1333.

Okada, M., Mimura, T., 1940. Zur Physiologie und Pharmakologie der Hartgewebe. IV. Mitteilung: Tagesrhythmus in der Knochenlamellenbildung. Proc. Japan Pharm. Soc., 95–97.

Reid, D.J., Dean, M.C., 2006. Variation in modern human enamel formation times. J. Hum. Evol. 50, 329–346.

Shinoda, H., Okada, M., 1988. Diurnal rhythms in the formation of lamellar bone in young growing animals. Proc. Japan Acad. 64 (Ser B), 307–310.

Smith, T.M., Reid, D.J., Dean, M.C., Olejniczak, A.J., Ferrell, R.J., Martin, L.B., 2007. New perspectives on chimpanzee molar crown development.

In: Bailey, S., Hublin, J.J. (Eds.), Dental Palaeoanthropology. Springer, Berlin, pp. 177–192.
Smolyar, I., Bromage, T.G., 2004. Discrete model of fish scale incremental pattern. A formalization of the 2D anisotropic structure. ICES J. Marine Sci. 61, 992–1003.
Vogel, C., Laing, M., Monnik, K., 2000. Drought in South Africa, with special reference to the 1980–94 period. In: Wilhite, D.A. (Ed.), Drought: a global assessment. Routledge Press, London, pp. 348–366.